Caprine Models of the Agonist-Antagonist Myoneural Interface Implemented at the Above- and Below-Knee Amputation Levels

Tyler R. Clites, Ph.D.
Matthew J. Carty, M.D.
Shriya S. Srinivasan, B.S.
Simon G. Talbot, M.D.
Rickard Brånemark, M.D., Ph.D.
Hugh M. Herr, Ph.D.

Cambridge and Boston, Mass.; and Gothenburg, Sweden

Background: Traditional approaches to amputation are not capable of reproducing the dynamic muscle relationships that are essential for proprioceptive sensation and joint control. In this study, the authors present two caprine models of the agonist-antagonist myoneural interface (AMI), a surgical approach designed to improve bidirectional neural control of a bionic limb. The key advancement of the AMI is the surgical coaptation of natively innervated agonist-antagonist muscle pairs within the residual limb.

Methods: One AMI was surgically created in the hindlimb of each of two African Pygmy goats at the time of primary transtibial amputation. Each animal was also implanted with muscle electrodes and sonomicrometer crystals to enable measurement of muscle activation and muscle state, respectively. Coupled agonist-antagonist excursion in the agonist-antagonist myoneural interface muscles was measured longitudinally for each animal. Fibrosis in the residual limb was evaluated grossly in each animal as part of a planned terminal procedure.

Results: Electromyographic and muscle state measurements showed coupled agonist-antagonist motion within the AMI in the presence of both neural activation and artificial muscle stimulation. Gross observation of the residual limb during a planned terminal procedure revealed a thin fibrotic encapsulation of the AMI constructs, which was not sufficient to preclude coupled muscle excursion.

Conclusions: These findings highlight the AMI's potential to provide coupled motion of distal agonist-antagonist muscle pairs preserved during below- or above-knee amputation at nearly human scale. Guided by these findings, it is the authors' expectation that further development of the AMI architecture will improve neural control of advanced limb prostheses through incorporation of physiologically relevant muscle-tendon proprioception. (*Plast. Reconstr. Surg.* 144: 218e, 2019.)

Advanced prosthetic limbs for persons with amputation have seen dramatic development in recent years,[1–7] including significant improvements in myoelectric control architectures.[1,6,8–11] However, natural reflection of joint position, speed, and torque sensations (called "proprioception") from a prosthetic limb onto the nervous system remains challenging.

From the Center for Extreme Bionics, Massachusetts Institute of Technology; the Division of Plastic Surgery, Brigham and Women's Hospital; and the Department of Orthopaedics, University of Gothenburg.
Received for publication June 20, 2018; accepted January 9, 2019.
Presented in part at the 62nd Annual Meeting of the Plastic Surgery Research Council, in Durham, North Carolina, May 4 through 7, 2017.

DOI: 10.1097/PRS.0000000000005864

Disclosure: *Dr. Herr has a consulting relationship with Ottobock. Dr. Brånemark is a consultant for Integrum AB, chairman of the board of Integrum AB, and his spouse is employed by Integrum Inc. Drs. Herr and Carty are inventors on an issued patent describing the AMI concept. Drs. Herr, Carty, and Clites are inventors on a pending patent describing the Ewing procedure. The Massachusetts Institute of Technology holds both patents. None of the other authors has a financial interest in any of the products or devices mentioned in this article.*

Proprioceptive feedback is mediated primarily by sensory organs within muscles and tendons.[12] A significant body of literature exists surrounding the biological structures involved in proprioceptive sensation, including stretch receptors in the skin[13–15] and movement receptors in the joints[16–18]; however, there is significant evidence highlighting muscle spindles and Golgi tendon organs[19] as the dominant mediators of joint proprioception.[12] Further evidence indicates that it is the dynamic relationships between sensory receptors within agonist-antagonist muscle pairs that drive natural neural sensations of joint movement.[20] The complexity of this afferent feedback system poses a challenging hurdle for the development of bionic limbs that are able to reflect natural proprioception onto the central nervous system.

The agonist-antagonist myoneural interface (AMI) has been described as a bidirectional neural communication paradigm capable of providing proprioceptive feedback from, and improving myoelectric control of, a prosthetic limb.[21–25] The AMI is composed of an agonist and an antagonist muscle connected mechanically in series, so that when the agonist contracts, the antagonist is stretched, and vice versa. The AMI is unique in its preservation of the dynamic muscle relationships that are fundamental to both joint control[26,27] and proprioceptive sensation.[12,20,28] Prior studies in a rat model have validated the AMI's potential to communicate neural signals of joint position, speed, and torque along native neural pathways by preserving biological mechanotransducers within each muscle.[23,24] However, because human musculoskeletal anatomy differs in both scale and morphology from that of the rat, exploration of AMI implementation at nearly human scale is prudent.

In this case study, we present, in two goats, a model for AMI construction during primary limb amputation at each of the below- and above-knee levels. We describe surgical techniques and muscular geometry of the AMI, highlighting differences in surgical approach that emerge between the two amputation levels. We also provide evidence of coupled agonist-antagonist muscle motion after a sustained period of healing. These results demonstrate the potential of the AMI to preserve dynamic agonist-antagonist muscle relationships at nearly human scale.

Supplemental digital content is available for this article. Direct URL citations appear in the text; simply type the URL address into any Web browser to access this content. Clickable links to the material are provided in the HTML text of this article on the *Journal*'s website (www.PRSJournal.com).

MATERIALS AND METHODS

Animals and Study Design

All animal care and procedures were conducted in accordance with the *Guide for the Care and Use of Laboratory Animals*,[29] and with approval from the Massachusetts Institute of Technology Committee on Animal Care (1214-130-17). This case study was designed to validate a surgical technique for implementation of the agonist-antagonist myoneural interface in below- and above-knee amputations (transtibial and transfemoral, respectively) at a nearly human scale. In a controlled surgical setting, two skeletally mature African pygmy goats (one 25-kg female goat and one 32.5-kg male goat) underwent unilateral hindlimb amputation at the transtibial level, with subsequent surgical remodeling of residual soft tissues.

The first goat (goat TT) served as a model for human transtibial amputation, in which all muscles necessary to create AMIs for the amputated ankle and subtalar joints originate proximal to the amputation site. In this setting, which closely mirrors the paradigm explored in prior rat studies,[23] AMIs can be created without proximal disinsertion of agonist-antagonist myoneural interface muscles by rerouting native agonist-antagonist muscle pairs across a pulley anchored to the tibia and coapting them at their distal ends (Fig. 1, *above*).

AMI creation at the above-knee level is more complex than at the below-knee level, because the ankle and subtalar musculature originates distal to the transfemoral amputation site. The second goat (goat TF) served as a model for human above-knee amputation; although the amputation for goat TF was performed at the transtibial level, the muscles responsible for ankle dorsi and plantar flexion were treated as they would be in an elective transfemoral amputation. In this setting, it is possible to isolate all relevant distal muscles as a series of independent neurovascular island flaps, and subsequently transpose these flaps proximally and incorporate them into the residual limb (Fig. 1, *below*). These flaps can then be manipulated and coapted to reinstate functional agonist-antagonist muscle relationships for control of

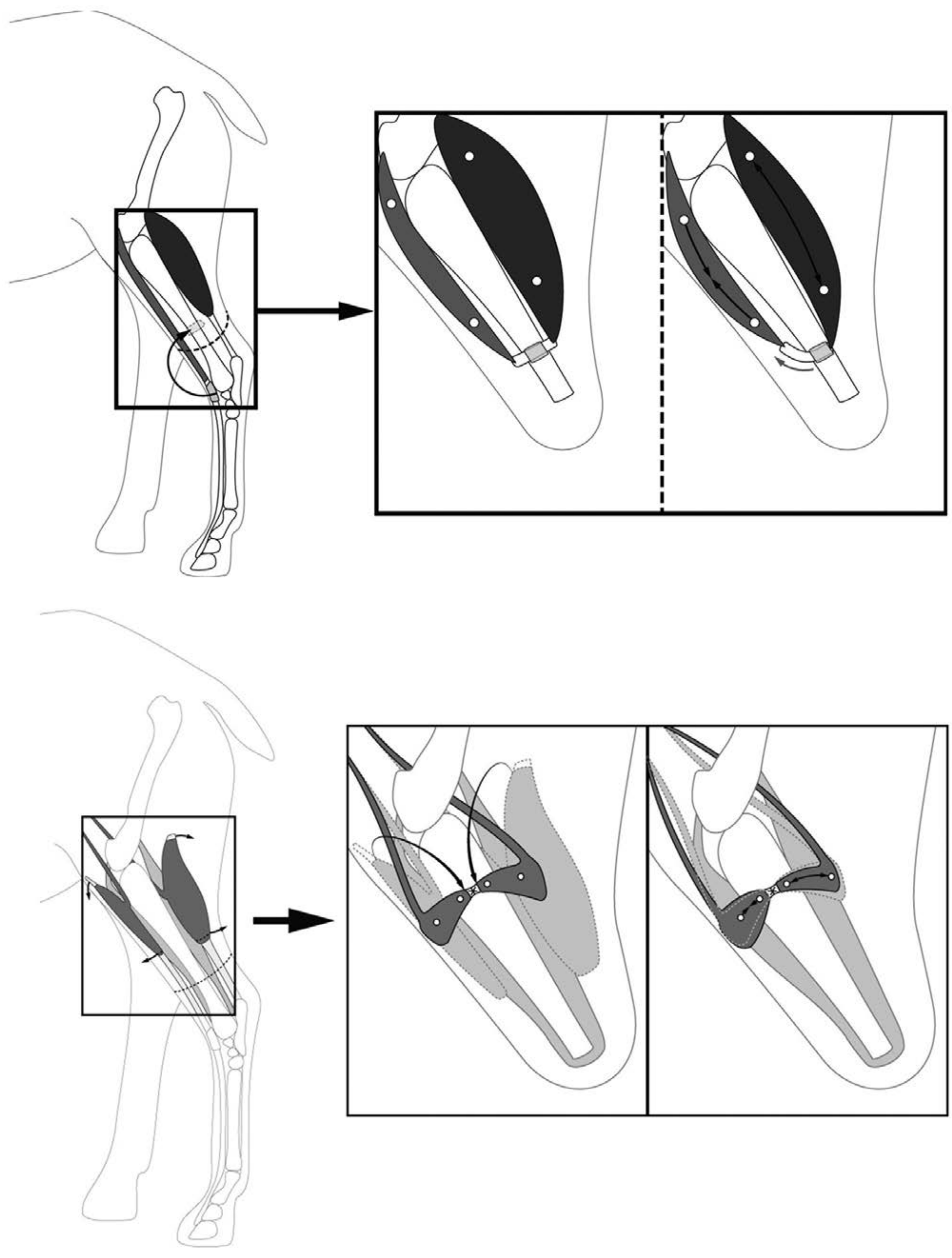

Fig. 1. Schematics of experimental amputation paradigm. (*Above*) In goat TT, native ankle flexor and extensor muscles in their native orientation are coapted to either end of a pulley affixed to the medial tibia, and constructed from a synovial canal harvested from the amputated ankle joint. (*Below*) In goat TF, each muscle is first isolated on its independent neurovascular leash. The two flaps are then coapted circumferentially around the residual limb, to form an AMI.

prosthetic ankle and subtalar joints. Because the knee flexor and extensor muscles originate proximal to the amputation site, AMIs for control of a prosthetic knee joint in a human patient can be constructed by rerouting native agonist-antagonist muscle pairs in situ, as described in the previous paragraph.

Preparation of Implanted Electronics

To facilitate chronic in vivo evaluation of AMI function, each goat was implanted with an assembly of indwelling muscle electrodes (Ardiem, East Indiana, Pa.) and sonomicrometer crystals (2-mm stainless steel; Sonometrics, London, Ontario, Canada). Sonomicrometry is a technique that uses ultrasound time-of-flight measurements from a pair of piezoelectric crystals to directly measure muscle length and speed.[30–32] The assembly implanted in goat TT consisted of four bipolar epimysial electrodes, two bipolar intramuscular electrodes, and four sonomicrometer crystals.[23,31,32] Before surgery, the leads from this array were bundled and their ends soldered to a circular connector (Omnetics, Minneapolis, Minn.). The base of this connector was coated with implantable silicone (NuSil, Carpinteria, Calif.) and housed in a custom three-dimensionally printed percutaneous skin port (Fig. 2, *above, left*). The skin port was printed from U.S. Pharmacopeia class VI implantable material (Stratasys, Eden Prairie, Minn.), and provided robust longitudinal access to the implanted components throughout the duration of the study.

The assembly implanted in goat TF was identical to that used in goat TT, with the exception of three additional bipolar epimysial electrodes. In goat TF, however, an osseointegrated implant was opted for in place of a skin port for percutaneous lead routing (Fig. 2, *above, right*, and *below*). This implant was a simplified version of the system first described in Ortiz-Catalan et al.[10] scaled appropriately for a goat. More detail on preparation of electrodes for the osseointegrated implant is provided in Supplemental Digital Content 1. (**See Document, Supplemental Digital Content 1**, which describes fabrication of the electrode lead bundle for the osseointegrated implant, and additional

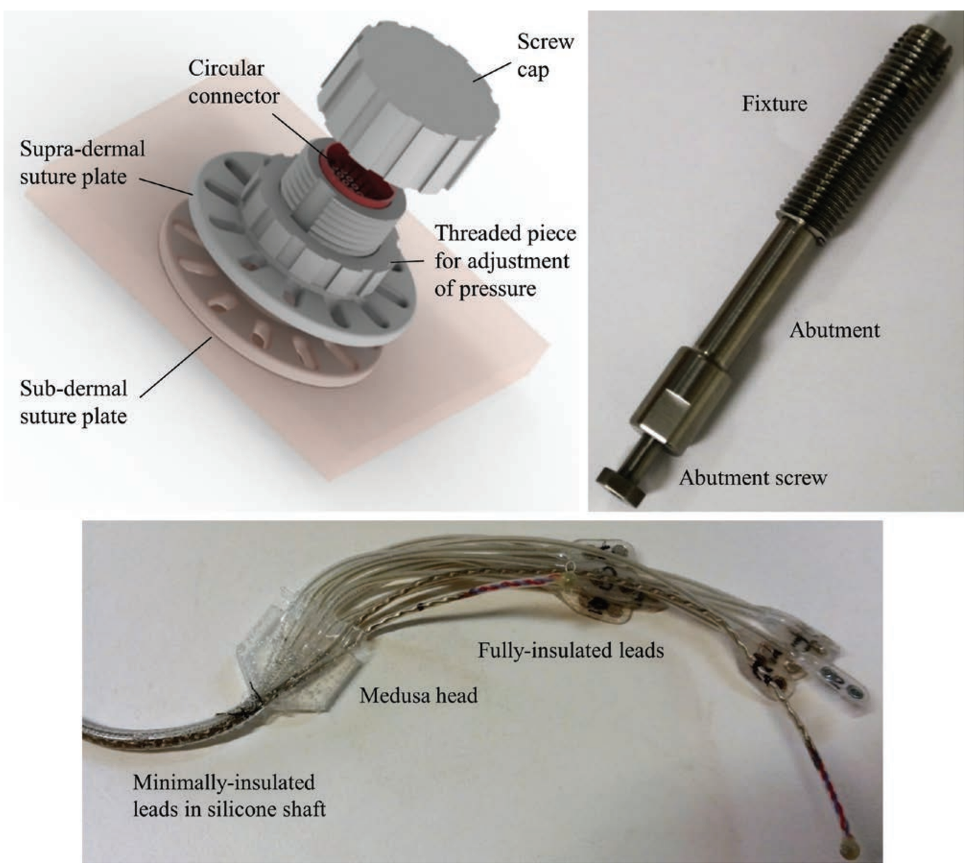

Fig. 2. Implanted components. (*Above*, *left*) The custom three-dimensionally printed percutaneous port developed for goat TT includes both a subdermal and a supradermal suture plate, which together compress the skin with an adjustable pressure. (*Above*, *right*) The osseointegrated implant developed for goat TF is a scaled, simplified version of the eOPRA system, which was first demonstrated in Ortiz-Catalan et al. (Ortiz-Catalan M, Håkansson B, Brånemark R. An osseointegrated human-machine gateway for long-term sensory feedback and motor control of artificial limbs. *Sci Transl Med*. 2014;6:257re6.) The system consists of an implanted fixture, a percutaneous abutment, and an abutment screw through which leads are routed. (*Below*) Constraints on combined diameter of percutaneously routed leads led to the incorporation of a "Medusa head" architecture.

details related to data processing, ***http://links.lww.com/PRS/D562***.)

Surgery

All amputation procedures were performed under sterile conditions, with the goat under general anesthesia and lying in the left lateral decubitus position. Both operations began with a distal circumferential incision in the midportion of the right leg, with a 10-cm anterior extension to the thigh. The skin envelope was elevated circumferentially, and dissection was carried down to the underlying muscle fascia of the superficial muscle compartment. The anterior and posterior leg compartments were explored to identify the tibialis cranialis, peroneus tertius, medial gastrocnemius, lateral gastrocnemius, and superficial digital flexor muscles. These muscles were marked at resting length tension with the ankle in the neutral position using multiple sutures set at 1-cm intervals. All muscles of the anterior superficial and deep posterior compartments were then disinserted.

In goat TT, dissection was then carried down to the level of the periosteum, and a tibial osteotomy was performed 4 cm proximal to the ankle joint. The anterior tibial, posterior tibial, and peroneal vessels were ligated, thus completing the amputation. The medial tarsal tunnel was procured from the distal amputated limb by means of sharp dissection, including a 3-cm segment of the tunnel's native tendon contents. The tunnel was then affixed to the medial flat of the residual limb tibia (Fig. 3, *above*, *left*) using multiple unicortical suture anchors. One AMI was constructed by means of coaptation of the tibialis cranialis and lateral gastrocnemius muscles to either end of the tendon portion passing through the tarsal tunnel (Fig. 3, *above*, *right*). A secondary incision was made for the skin port in the left haunch, and the electrode bundle was passed subcutaneously to the primary surgical site (Fig. 3, *below*). Electrodes and crystals were affixed in the following locations and quantities, using 4-0 Vicryl (Ethicon, Inc., Somerville, N.J.) suture: tibialis cranialis (one intramuscular and two epimysial, and three crystals), lateral gastrocnemius (one intramuscular and one epimysial, and two crystals), and tibial tuberosity (one epimysial, as an electrical reference). The soft-tissue envelope was closed in a layered fashion using 3-0 Monocryl (Ethicon) intradermal sutures and 4-0 Monocryl subcuticular running sutures. The limb was dressed with a lightly wrapped modified Robert Jones bandage.

In goat TF, the AMI was constructed before the tibial osteotomy was performed. The primary neurovascular supply to the peroneus tertius and lateral gastrocnemius were exposed and isolated. The peroneus tertius was disinserted both proximally and distally, creating a neurovascular island flap (Fig. 4, *above*, *left*). The lateral gastrocnemius was isolated from the medial gastrocnemius, and disinserted both proximally and distally. The lateral gastrocnemius was rotated 90 degrees clockwise from its native orientation, and the peroneus tertius was rotated 90 degrees counterclockwise, with care taken to avoid stressing the neurovascular leash of either muscle. The lateral gastrocnemius was tunneled beneath the hip flexor, but superficial to the medial gastrocnemius and superficial digital flexor. The peroneus tertius and lateral gastrocnemius tendons were then coapted both laterally (origin-to-origin) (Fig. 4, *above*, *right*) and medially (insertion-to-insertion) (Fig. 4, *below*, *left*) by means of modified Kessler repair technique using 3-0 Ethibond (Ethicon) sutures to create a single circumferential AMI unit. Coaptation was performed with each muscle at its resting tension. A tibial osteotomy was then performed 9 cm proximal to the ankle joint, and the osseointegrated fixture was placed as described previously.[33] Electrode leads were passed through a cortical window drilled 8 cm proximal to the site of the osteotomy, and routed out the distal end of the bone, through the osseointegrated implant (Fig. 4, *below*, *right*). (**See Figure, Supplemental Digital Content 2**, which shows a wire bundle exiting the osseointegrated implant. Continuity was confirmed, and electrode leads were identified and labeled intraoperatively, after passage of the lead bundle through the abutment screw, ***http://links.lww.com/PRS/D563***.) The bundle of electrode leads, or Medusa head, shown in Figure 2, *below*, *left*, was secured to the anterior tibial periosteum using 4-0 Prolene (Ethicon) sutures. Electrodes and crystals were affixed in the following locations and quantities, using 4-0 Vicryl suture: peroneus tertius (one intramuscular and one epimysial, and two crystals), lateral gastrocnemius (one intramuscular and one epimysial, and two crystals), superficial digital flexor (one epimysial), tibialis cranialis (one epimysial), medial gastrocnemius (one epimysial), and tibial tuberosity (two epimysial). A muscle platform was constructed at the base of the tibia, and the distal skin flap was anchored to this platform.[33] The remainder of the soft-tissue envelope was closed in a layered fashion using 3-0 Monocryl intradermal sutures and 4-0 Monocryl subcuticular

Fig. 3. Goat TT surgical technique. (*Above*, *left*) One tarsal tunnel is harvested from the amputated ankle joint, with internal tendon intact, and fixed to the medial tibia using suture anchors. (*Above*, *right*) Tibialis cranialis and lateral gastrocnemius are coapted to either end of the synovial canal tendon. (*Below*, *left*) The skin port is sutured in place on the right haunch. (*Below*, *right*) Electrodes are visible on plain radiography. *LG*, lateral gastrocnemius; *TC*, tibialis cranialis.

running sutures. The limb was dressed with a lightly wrapped Robert Jones bandage, with a rigid distal cap to prevent premature loading of the osseointegrated implant. At postoperative day 7, with the animal under sedation, the bandage was removed while a circular connector (Omnetics, Minneapolis, Minn.) was soldered to the wires exiting the osseointegrated implant. The wire exit was then sealed with injectable dental cement and reinforced with heat-shrink tubing.

Data Collection and Processing

To assess coupled motion of the AMI construct in goat TT, electromyography and sonomicrometry signals were recorded simultaneously while the animal walked freely in a confined area. Muscle stretch measurements from the tibialis cranialis, obtained by means of sonomicrometry, were cross-correlated with the differential electromyography in the plantar-flexion direction (i.e., electromyography of the lateral gastrocnemius minus electromyography of the tibialis cranialis).

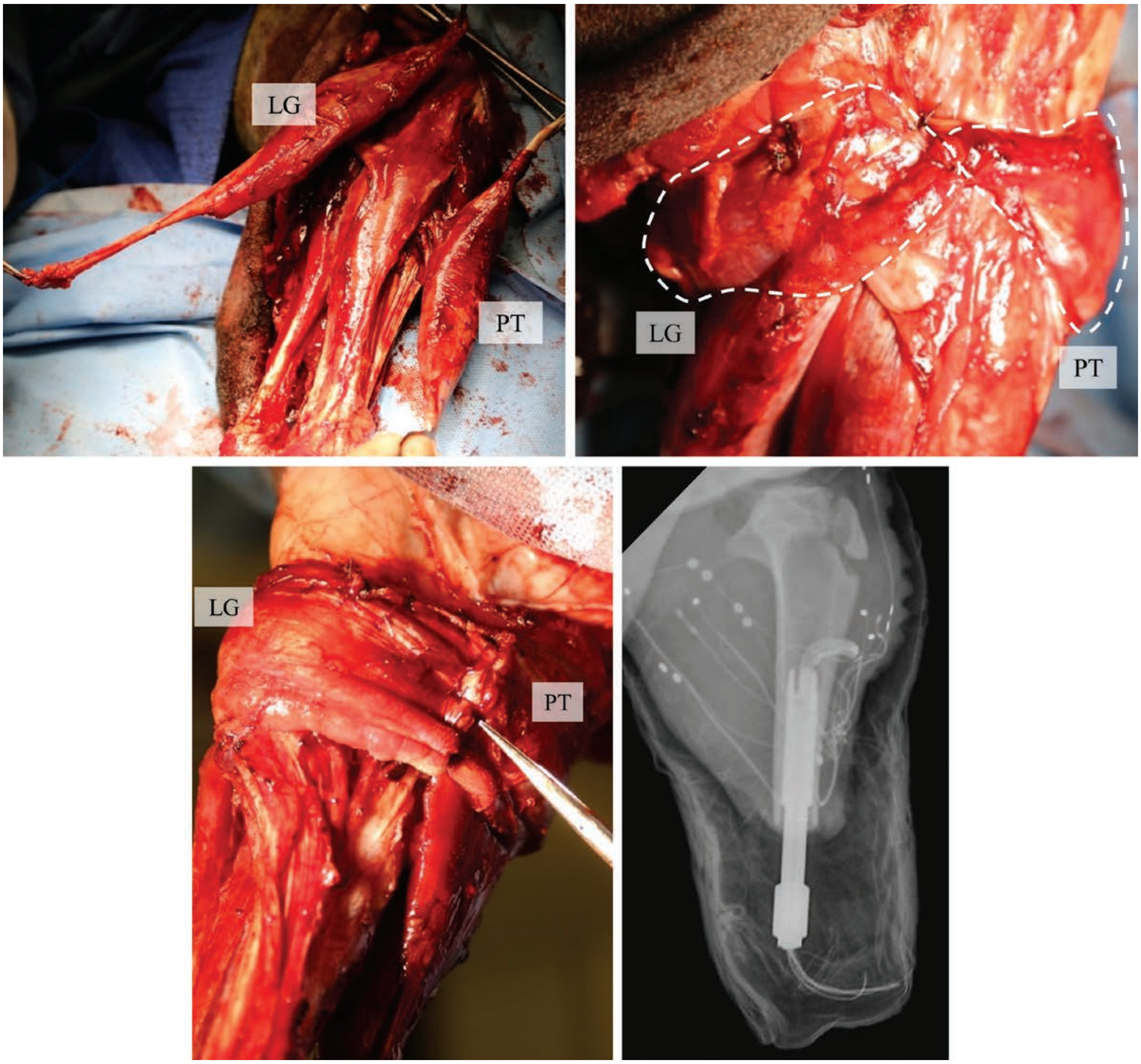

Fig. 4. Surgical technique used for goat TF. (*Above*, *left*) The lateral gastrocnemius and peroneus tertius are isolated on their neurovascular leashes. (*Above*, *right*) The lateral gastrocnemius and peroneus tertius are each rotated 90 degrees and coapted at their origins. (*Below*, *left*) Both muscles are wrapped circumferentially around the limb, shortened, and coapted on the medial side of the limb, at their distal ends. (*Below*, *right*) Leads are routed percutaneously, through the osseointegrated implant. Crystals, electrodes, and the osseointegrated implant are all visible in plain radiography. *LG*, lateral gastrocnemius; *PT*, peroneus tertius.

In a second experiment, with goat TT under sedation and in the left lateral decubitus position, an artificial stimulus (50 Hz, 2 mA, and 500 μsec) was applied to the tibialis cranialis while muscle stretch was recorded from both the tibialis cranialis and the lateral gastrocnemius. Both experiments were conducted at postoperative day 60.

Because goat TF's connector port was located in the distal end of his osseointegrated implant, it was difficult to maintain a stable connection to the implanted components while he was ambulatory. For this reason, data were collected only with goat TF under sedation and in the left lateral decubitus position. In this experiment, an artificial stimulus (50 Hz) was applied to the peroneus tertius, as muscle stretch was recorded from the lateral gastrocnemius. Stimulus amplitude and pulse width were modulated to control lateral gastrocnemius muscle stretch.[23] This experiment was conducted at postoperative day 30.

Terminal Surgery and Gross Tissue Examination

At postoperative day 60, a planned terminal procedure was carried out in goat TT, during which the limb was evaluated grossly for scarring and adhesion. Goat TF had an unexpected

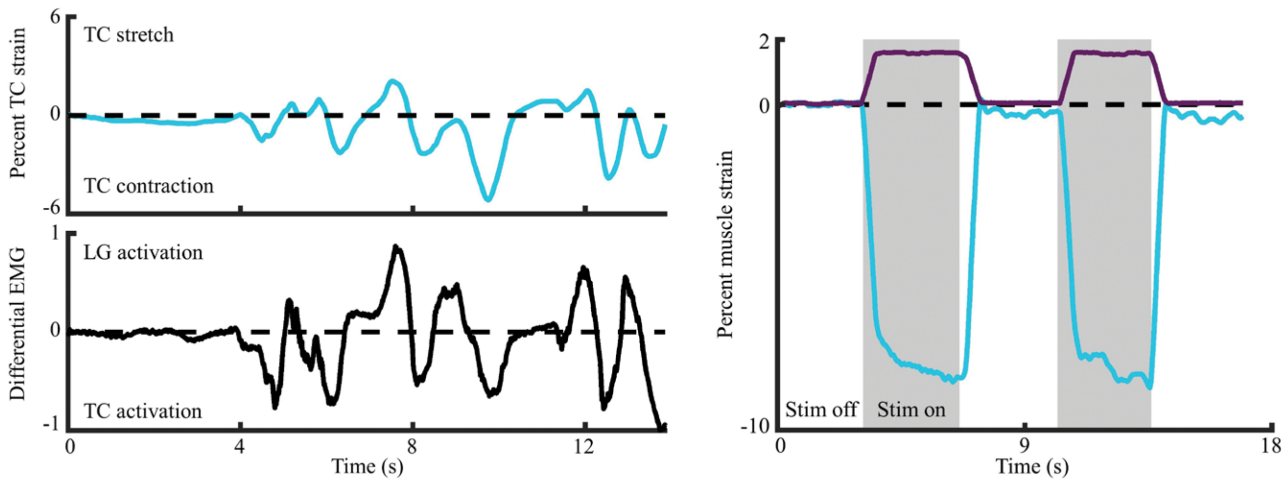

Fig. 5. Coupled AMI motion in goat TT. (*Left*) Tibialis cranialis strain correlates with differential electromyography (electromyography of the lateral gastrocnemius minus electromyography of the tibialis cranialis) during ambulation. (*Right*) lateral gastrocnemius muscle strain (*purple*) correlates inversely with tibialis cranialis muscle strain (*light blue*) during artificial stimulation of the tibialis cranialis. Both experiments were conducted at postoperative day 60. *TC*, tibialis cranialis; *LG*, lateral gastrocnemius; *EMG*, electromyography.

tendency to load the distal end of the implant while he walked, putting strain on the wire leads that eventually led to breakage, causing a loss of connectivity with the implanted hardware at approximately postoperative day 90. However, the goat remained healthy, and a planned terminal procedure was carried out at postoperative day 447. During this terminal procedure, in addition to gross tissue evaluation, the exposed muscles were stimulated to assess coupled motion of the AMI. Because electrode and crystal leads could no longer be accessed, stimulus was delivered by means of an external hook electrode held in contact with the muscle surface (50 Hz, 8 mA, and 500 μsec). Muscle excursion was measured by tracking a pair of metal staples placed acutely on the surface of the peroneus tertius and lateral gastrocnemius.

RESULTS

Below-Knee Surgical Model

At postoperative day 60, tibialis cranialis muscle stretch in goat TT correlated positively with differential plantar-flexion activation during ambulation (Fig. 5, *left*) (Pearson coefficient, $R = 0.67$; $p < 0.000001$ for correlation), implying coupled motion within the AMI. With the animal sedated, under artificial stimulation of the tibialis cranialis, lateral gastrocnemius muscle strain correlated inversely with tibialis cranialis muscle strain (Fig. 5, *right*) (Pearson coefficient, $R = -0.99$; $p < 0.000001$ for correlation), further evidencing a functional mechanical linkage between the two AMI muscles. On gross evaluation of the residual limb during the terminal dissection, there was a thin fibrotic capsule surrounding the construct. Heavy adhesions were isolated to the lateral aspect of the limb, with foci around the implanted components and the distal medial gastrocnemius into the Achilles, which was split off from the lateral gastrocnemius at the time of surgery and isolated for coverage. The synovial pulley was still intact; further dissection into the canal revealed a scar-free lubricious interface between the internal tendon and surrounding synovium.

Above-Knee Surgical Model

At postoperative day 30, lateral gastrocnemius strain was modulated in goat TF by varying stimulation of the peroneus tertius (Fig. 6, *left*). Because of time restrictions associated with sedation, it was not possible to optimize performance of the closed-loop stimulation controller. However, previous literature has shown that improved performance may be possible with proper tuning of the stimulation controller gains.[23] At postoperative day 447, during a planned terminal procedure, the skin envelope was retracted, with care taken to not disrupt any scarring that may have formed overlying the AMI construct. With the skin retracted, a stimulus applied to the lateral gastrocnemius elicited stretch in the peroneus tertius (Fig. 6, *right*), indicating coupled

Video 1. Supplemental Digital Content 3 demonstrates coupled motion of the AMI muscles during artificial stimulation. With the skin envelope open, passive stretch of the AMI agonist (peroneus tertius) was visualized during functional electrical stimulation of the antagonist (lateral gastrocnemius), ***http://links.lww.com/PRS/D564***.

Video 2. Supplemental Digital Content 4 demonstrates manual excursion of the AMI construct. Passive manual excursion of the AMI's coaptation point demonstrates the ability of the AMI construct to slide relative to the underlying tissue, ***http://links.lww.com/PRS/D565***.

motion of the agonist-antagonist myoneural interface. [**See Video, Supplemental Digital Content 3**, which demonstrates coupled motion of the AMI muscles during artificial stimulation. With the skin envelope open, passive stretch of the AMI agonist (peroneus tertius) was visualized during functional electrical stimulation of the antagonist (lateral gastrocnemius), ***http://links.lww.com/PRS/D564***.] On gross evaluation, the AMI construct was encapsulated in fibrotic tissue, but this was not sufficient to inhibit sliding of the AMI. The coaptation point between the two AMI muscles was intact (Fig. 7, *left*). Light force applied with forceps to one of the AMI muscles was sufficient to manually excurse the coaptation point relative to the underlying tissues. (**See Video, Supplemental Digital Content 4**, which demonstrates manual excursion of the agonist-antagonist myoneural interface construct. Passive manual excursion of the AMI's coaptation point demonstrates the ability of the AMI construct to slide relative to the underlying tissue, ***http://links.lww.com/PRS/D565***.) Further dissection revealed the development of a fascial plane deep to the AMI muscles, separating the AMI from the underlying tissues (Fig. 7, *right*).

Although ancillary to the AMI study, it is worth reporting that the percutaneous osseointegrated implant remained stable and infection-free throughout the duration of the study. At postoperative day 190, goat TF was fitted with a passive bone-anchored prosthesis, and was able to ambulate freely within a confined space. [**See Figure, Supplemental Digital Content 5**, which shows healing of osseointegrated implant. (*Left*) At postoperative day 190, there is a robust skin seal around the osseointegrated implant. (*Right*) Goat TF was able to ambulate within a confined space while wearing a passive transtibial prosthesis (Prilutsky Lab, Georgia Tech, Atlanta, Ga.), ***http://links.lww.com/PRS/D566***.]

DISCUSSION

This case study presents a longitudinal exploration of surgical architectures for the agonist-antagonist myoneural interface in two goats. In both animals, the AMI constructs showed evidence of coupled agonist-antagonist motion throughout the duration of the experiments. Unsurprisingly, fibrotic adhesions were present in the posthealing residual limb of both animals; however, these adhesions were not sufficient in either animal to preclude coupled motion of the AMI. Because the surgical models here presented were each limited to a single animal, these data are not sufficient to rule out the possibility of scarring; instead, they highlight the AMI's potential to reinstate coupled agonist-antagonist muscle relationships at a nearly human scale. Future studies in larger populations will be conducted to ensure that the AMI is able to reproduce sufficient levels of agonist-antagonist muscle excursion to elicit useful sensations of joint movement.

A significant portion of the learning derived from this experimental work was associated with

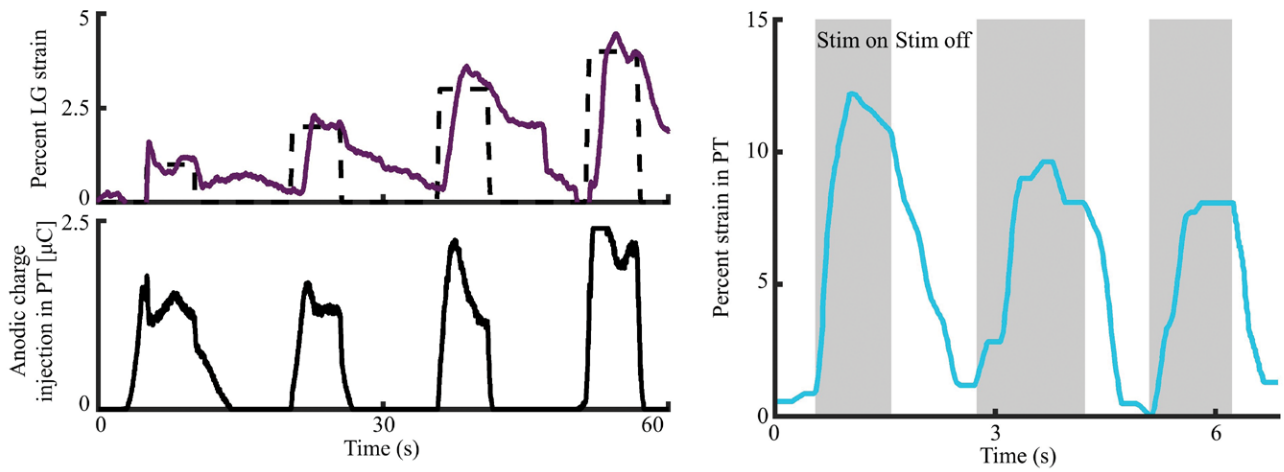

Fig. 6. Coupled AMI motion in goat TF. (*Left*) At postoperative day 30, lateral gastrocnemius strain is modulated by varying the intensity of artificial stimulation delivered to the peroneus tertius. (*Right*) At postoperative day 447, with the residual limb open, strain is induced in the peroneus tertius by means of artificial stimulation of the lateral gastrocnemius. *PT*, peroneus tertius; *LG*, lateral gastrocnemius.

designing implant architectures that would survive longitudinal implantation in unruly quadrupeds. The solutions presented were sufficiently robust to withstand the wear-and-tear of caprine life, with the exception of the leads routed through the percutaneous osseointegrated implant.

The AMI's primary purpose is to improve bidirectional control of myoelectric prosthetic limbs.[25] Such prosthetic devices are becoming increasingly common in the upper extremity, with the advent of commercial pattern-recognition–based myoelectric control systems (e.g., Coapt, LLC, Chicago, Ill.). Although commercially available lower extremity robotic prostheses, such as the Power Knee (Ossur, Reykjavik, Iceland) or the emPOWER ankle (Ottobock, Duderstadt, Germany), are not currently designed for myoelectric control, the technology necessary to upgrade these systems to use electromyography as a control signal has been demonstrated[1,25] and may be available commercially in the near future. In addition, preliminary studies indicate that there may be clinical benefits to the AMI even in the absence of a myoelectric prosthesis, such as attenuation of residual limb atrophy or reduction in aberrant phantom sensation.[34] These benefits may motivate adoption of the AMI even before next-generation prosthetic devices become broadly available.

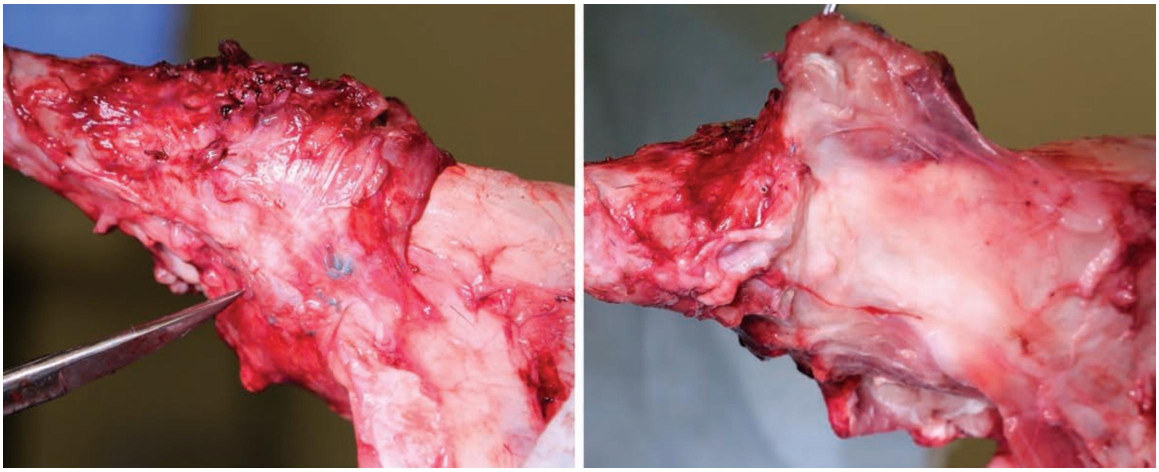

Fig. 7. Healing in goat TF residual limb. (*Left*) At postoperative day 447, the AMI coaptation point is still intact. (*Right*) Further dissection reveals a lubricious fascial layer separating the AMI from underlying tissues.

The results of this case study provide evidence toward the scalability of the agonist-antagonist myoneural interface concept, which has been previously demonstrated in rat studies. The approaches here presented assume access to distal musculature with native innervation and vascular supply. As such, the specific surgical methodologies explored in this article may not be applicable in the setting of a preexisting amputation, which means that adoption of these procedures would require a reframing of the index amputation procedure. Modifications to the proposed procedures would also be necessary in primary amputation cases where there is significant damage to the distal soft tissues. However, by leveraging regenerative properties of muscle and nerve tissues, it may be possible to expand the reach of the AMI to patients in whom distal tissues are compromised or have already been amputated.[24,35]

CONCLUSIONS

In this article, we describe surgical architectures for nearly human scale implementation of the AMI at each of the below- and above-knee amputation levels. By offering the possibility of higher fidelity control and the restoration of proprioceptive sensation, the AMI has the potential to improve function and quality of life for persons with amputation.

Hugh M. Herr, Ph.D.
Center for Extreme Bionics
Massachusetts Institute of Technology Media Lab
75 Amherst Street
Cambridge, Mass. 02139
hherr@media.mit.edu

REFERENCES

1. Hargrove LJ, Simon AM, Young AJ, et al. Robotic leg control with EMG decoding in an amputee with nerve transfers. *N Engl J Med.* 2013;369:1237–1242.
2. Rouse EJ, Hargrove LJ, Perreault EJ, Kuiken TA. Estimation of human ankle impedance during the stance phase of walking. *IEEE Trans Neural Syst Rehabil Eng.* 2014;22:870–878.
3. Herr HM, Grabowski AM. Bionic ankle-foot prosthesis normalizes walking gait for persons with leg amputation. *Proc Biol Sci.* 2012;279:457–464.
4. Bellman RD, Holgate MA, Sugar TG. SPARKy 3: Design of an active robotic ankle prosthesis with two actuated degrees of freedom using regenerative kinetics. In: *Proceedings of the 2nd Biennial IEEE/RAS-EMBS International Conference on Biomechanical Robotics and Biomechatronics.* Piscataway, NJ: IEEE Xplore; 2009:511–516.
5. Sup F, Bohara A, Goldfarb M. Design and control of a powered transfemoral prosthesis. *Int J Rob Res.* 2008;27:263–273.
6. Huang S, Wensman JP, Ferris DP. An experimental powered lower limb prosthesis using proportional myoelectric control. *J Med Device* 2014;8:024501-1–024501-2.
7. Huang H, Kuiken TA. A strategy for identifying locomotion modes using surface electromyography. *IEEE Trans Biomed Eng.* 2009;56:65–73.
8. Hargrove LJ, Simon AM, Lipschutz RD, Finucane SB, Kuiken TA. Real-time myoelectric control of knee and ankle motions for transfemoral amputees. *JAMA* 2011;305:1542–1544.
9. Kuiken TA, Li G, Lock BA, et al. Targeted muscle reinnervation for real-time myoelectric control of multifunction artificial arms. *JAMA* 2009;301:619–628.
10. Ortiz-Catalan M, Håkansson B, Brånemark R. An osseointegrated human-machine gateway for long-term sensory feedback and motor control of artificial limbs. *Sci Transl Med.* 2014;6:257re6.
11. Irwin ZT, Schroeder KE, Vu PP, et al. Chronic recording of hand prosthesis control signals via a regenerative peripheral nerve interface in a rhesus macaque. *J Neural Eng.* 2016;13:046007.
12. Proske U, Gandevia SC. The proprioceptive senses: Their roles in signaling body shape, body position and movement, and muscle force. *Physiol Rev.* 2012;92:1651–1697.
13. Ochoa J, Torebjörk E. Sensations evoked by intraneural microstimulation of single mechanoreceptor units innervating the human hand. *J Physiol.* 1983;342:633–654.
14. Macefield G, Gandevia SC, Burke D. Perceptual responses to microstimulation of single afferents innervating joints, muscles and skin of the human hand. *J Physiol.* 1990;429:113–129.
15. Collins DF, Refshauge KM, Todd G, Gandevia SC. Cutaneous receptors contribute to kinesthesia at the index finger, elbow, and knee. *J Neurophysiol.* 2005;94:1699–1706.
16. Boyd IA, Roberts TD. Proprioceptive discharges from stretch-receptors in the knee-joint of the cat. *J Physiol.* 1953;122:38–58.
17. Skoglund S. Anatomical and physiological studies of knee joint innervation in the cat. *Acta Physiol Scand Suppl.* 1956;36:1–101.
18. Burke D, Gandevia SC, Macefield G. Responses to passive movement of receptors in joint, skin and muscle of the human hand. *J Physiol.* 1988;402:347–361.
19. Jami L. Golgi tendon organs in mammalian skeletal muscle: Functional properties and central actions. *Physiol Rev.* 1992;72:623–666.
20. Ribot-Ciscar E, Roll JP. Ago-antagonist muscle spindle inputs contribute together to joint movement coding in man. *Brain Res.* 1998;791:167–176.
21. Herr HM, Riso RR, Song KW, Casler RJ, Carty MJ. Peripheral neural interface via nerve regeneration to distal tissues. US patent 20160346099. January 1, 2016.
22. Herr HM, Clites TR, Maimon B, Zorzos A, Carty MJ, Duval JF. Method and system for providing proprioceptive feedback and functionality mitigating limb pathology. US patent application 62/276422. February 1, 2016.
23. Clites TR, Carty MJ, Srinivasan S, Zorzos AN, Herr HM. A murine model of a novel surgical architecture for proprioceptive muscle feedback and its potential application to control of advanced limb prostheses. *J Neural Eng.* 2017;14:036002.
24. Srinivasan SS, Carty MJ, Calvaresi PW, et al. On prosthetic control: A regenerative agonist-antagonist myoneural interface. *Sci Robot.* 2017;2:eaan2971.
25. Clites TR, Carty MJ, Ullauri JB, et al. Proprioception from a neurally controlled lower-extremity prosthesis. *Sci Transl Med.* 2018;10:eaap8373.
26. Hogan N. Adaptive control of mechanical impedance by coactivation of antagonist muscles. *IEEE Trans Automat Contr.* 1984;29:681–690.

27. Edwards WT. Effect of joint stiffness on standing stability. *Gait Posture* 2007;25:432–439.
28. Dimitriou M. Human muscle spindle sensitivity reflects the balance of activity between antagonistic muscles. *J Neurosci.* 2014;34:13644–13655.
29. National Research Council. *Guide for the Care and Use of Laboratory Animals*. Washington, DC: National Academies Press; 2011.
30. Griffiths RI. Ultrasound transit time gives direct measurement of muscle fibre length in vivo. *J Neurosci Methods* 1987;21:159–165.
31. Roberts TJ, Marsh RL, Weyland PG, Taylor CR. Muscular force in running turkeys: The economy of minimizing work. *Science* 1997;275:1113–1115.
32. McGuigan MP, Yoo E, Lee DV, Biewener AA. Dynamics of goat distal hind limb muscle-tendon function in response to locomotor grade. *J Exp Biol.* 2009;212:2092–2104.
33. Integrum AB. OPRA Implant System instructions for use. Available at: https://www.accessdata.fda.gov/cdrh_docs/pdf8/H080004D.pdf. Accessed September 12, 2016.
34. Clites TR, Herr HM, Srinivasan SS, Zorzos AN, Carty MJ. The Ewing amputation: The first human implementation of the agonist-antagonist myoneural interface. *Plast Reconstr Surg Global Open* 2018;6:e1997.
35. Kung TA, Langhals NB, Martin DC, Johnson PJ, Cederna PS, Urbanchek MG. Regenerative peripheral nerve interface viability and signal transduction with an implanted electrode. *Plast Reconstr Surg.* 2014;133:1380–1394.